



Published in final edited form as:

FEBS J. 2018 February ; 285(3): 467–480. doi:10.1111/febs.14351.

14-3-3 proteins mediate inhibitory effects of cAMP on salt-inducible kinases (SIKs)

Tim Sonntag¹, Joan M. Vaughan¹, and Marc Montminy^{1,*}

¹Clayton Foundation Laboratories for Peptide Biology, The Salk Institute for Biological Studies, La Jolla, California 92037, USA

Abstract

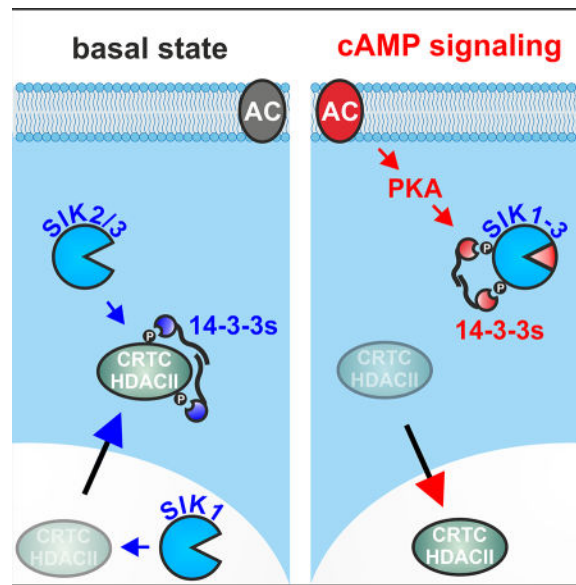
The salt-inducible kinase (SIK) family regulates cellular gene expression via the phosphorylation of cAMP-responsive transcriptional coactivators (CRTC) and class IIA histone deacetylases (HDACs), which are sequestered in the cytoplasm by phosphorylation-dependent 14-3-3 interactions. SIK activity towards these substrates is inhibited by increases in cAMP signaling, although the underlying mechanism is unclear. Here we show that the PKA-dependent phosphorylation of SIKs inhibits their catalytic activity by inducing 14-3-3 protein binding. SIK1 and SIK3 contain two functional PKA/14-3-3 sites, while SIK2 has four. In keeping with the dimeric nature of 14-3-3s, the presence of multiple binding sites within target proteins dramatically increases binding affinity. As a result, loss of a single 14-3-3 binding site in SIK1 and SIK3 abolished 14-3-3 association and rendered them insensitive to cAMP. By contrast, mutation of three sites in SIK2 were necessary to fully block cAMP regulation. Superimposed on effects of PKA phosphorylation and 14-3-3 association, an evolutionary conserved domain in SIK1 and SIK2 (the so called RK-rich region; 595–624 in hSIK2) is also required for inhibition of SIK2 activity. Collectively, these results point to a dual role for 14-3-3 proteins in repressing a family of Ser/Thr kinases as well as their substrates.

Graphical abstract

*To whom correspondence should be addressed. montminy@salk.edu.

Author Contributions

TS designed and performed the experiments, analyzed data, and wrote the manuscript. JMV generated the phospho-SIK1 S575 antiserum. MM designed the study and reviewed/edited the manuscript. All authors reviewed results and approved the final version of the manuscript.



Scheme depicting the interplay of the SIK kinases with their canonical substrates cAMP-regulated transcriptional coactivators (CRTCs) and class IIA histone deacetylases (HDACs). Under basal conditions, SIK-mediated phosphorylation sequesters CRTCs/HDACs in the cytoplasm by inducing 14-3-3 binding. Upon cAMP stimulation, PKA-mediated phosphorylation inactivates the SIKs via 14-3-3 dimer association. In consequence, CRTCs/HDACs are dephosphorylated, lose 14-3-3s, and translocate to the nucleus.

Keywords

14-3-3 protein; catalytic activity; transcriptional regulation; protein phosphorylation

Introduction

The AMP-activated protein kinase (AMPK) family of Ser/Thr kinases comprises 14 members, including the sub-family of salt-inducible kinases (SIKs), which are primarily activated by the master kinase LKB1 (STK11) [1, 2]. The three SIK members (SIK1–3) recognize substrates containing a common LXBS/TXSXXXL motif (underlined = phosphorylated residue, B = basic amino acid, and X = any residue), thereby regulating metabolism, cellular growth/survival, inflammation, and sleep [2–8]. In keeping with the proposed role of LKB1 as the AMPK family master kinase, SIK activity is abolished in cell lines and mice with a knockout of LKB1 [1, 9].

Perhaps the best understood substrates of SIK1–3 are the cAMP-regulated transcriptional coactivators (CRTCs; CRTC1–3) and class IIA histone deacetylases (HDACs; HDAC4,5,7,9) [3, 7]. Class IIA HDACs repress myogenesis and osteogenesis following their recruitment to target genes such as myocyte enhancer factors 2 (MEF2) and sclerostin (SOST) [3, 8]. CRTCs stimulate cAMP-responsive target genes by interacting with members of the cAMP response-element binding protein (CREB) transcription factors (ATF1, CREB, and CREM) [10]. SIKs phosphorylate multiple sites inside both CRTCs and class IIA

HDACs, which serve as phosphorylation-dependent 14-3-3 binding sites that sequester both protein families inside the cytoplasm [7, 11–16]. In this way, SIKs and 14-3-3s control the nuclear to cytoplasmic shuttling and hence transcriptional activity of CRTCs and HDACs.

14-3-3 proteins are conserved regulatory molecules that exist predominantly as dimers [17–19]. Generally, 14-3-3s associate with phosphorylated ligands containing either mode I (RSXSXP) or mode II (RXXXSXP; underlined = phosphorylated residue, and X = any residue) consensus recognition motifs [20, 21]. In keeping with the dimeric form of 14-3-3 proteins, synthetic ligands that incorporate two 14-3-3 consensus motifs show substantially higher 14-3-3 binding affinity (~30-fold) than ligands with only one motif [22]. Many proteins contain a primary high affinity or “gatekeeper” site and secondary low affinity sites [21, 23]. These dimeric 14-3-3 interactions are thought to induce large conformational changes within the target protein that can affect subcellular localization or catalytic activity [17, 21, 24].

The second messenger cAMP stimulates cellular gene expression via the activation of protein kinase A (PKA), which in turn phosphorylates CREB as well as the SIKs [10, 25]. CREB phosphorylation induces its transcriptional activity by promoting an association with the histone acetyltransferases CREB-binding protein (CBP) and P300 [26]. By contrast, PKA-mediated phosphorylation of the SIKs disrupts their catalytic activity by an unknown mechanism [10]. Although non-phosphorylatable PKA site mutants of SIK1 to SIK3 are insensitive to cAMP/PKA signaling in cell-based assays, PKA does not appear to block SIK1 or SIK2 activity *in vitro* [3, 27–31]. Based on previous studies documenting the interaction of SIKs with 14-3-3 proteins, we systematically investigated the 14-3-3 binding patterns of each SIK family member [27, 28, 32, 33]. We found that 14-3-3 proteins bind to all three SIKs in a PKA-dependent manner, leading to the inhibition of SIK1–3 activity both *in vivo* and *in vitro*. Our results point to a conserved molecular mechanism by which cAMP modulates cellular gene expression across vertebrates.

Results

SIK activity is inhibited by cAMP signaling

cAMP inhibits the SIK family by PKA-mediated phosphorylation, leading to the dephosphorylation, liberation from 14-3-3 proteins, and nuclear translocation of CRTCs (Fig. 1A). In studies of HEK293T cells, overexpression of SIK1–3 enhanced the phosphorylation of CRTC2/3 at two conserved SIK phosphorylation sites (S171 and S275 of CRTC2) that mediate cooperative binding of CRTCs to 14-3-3 proteins (Fig. 1B) [14]. Consistent with the inhibitory effect of cAMP/PKA on SIK activity, short-term exposure to the adenylyl cyclase activator Forskolin (Fsk) triggered the dephosphorylation of CRTC2/3, in control and SIK1–3 overexpressing HEK-293T cells. In keeping with its short half-life, protein amounts of overexpressed SIK1 were decreased in comparison to SIK2 and SIK3 [34].

We employed a transient CRE based reporter assay to monitor the inhibition of CRTC transcriptional activity by SIKs (Fig. 1C & 1D). This assay measures cAMP-dependent transcription, by expressing the luciferase gene under the control of a promoter containing

CREB binding sites, referred to as cAMP-response elements (CREs) [35]. Overexpression of CRTCs alone augmented CRE reporter activity constitutively, while coexpression of SIK1–3 effectively suppressed the CRE reporter (CRTC1 = ~25% and CRTC2/3 = ~5% CRE reporter activity; Fig. 1C). By contrast with the inhibitory effects of wild type SIK2, catalytically inactive SIK2 T175A mutant (Ala substitution at the critical LKB1 phosphorylation site) had less pronounced effects on CRTC activity (CRTC2 & SIK2 = ~5% and CRTC2 & SIK2 T175A = ~45% CRE reporter activity; Fig. 1C). Consistent with its ability to inactivate SIKs, exposure to Fsk stimulated the activities of CRTC2 and CRTC3 (CRTC1 & SIK1–3 = ~2-fold and CRTC2/3 & SIK1–3 = 10 to 30-fold change upon Fsk treatment; Fig. 1D). Despite its lower accumulation in transfected cells, SIK1 repressed CRTC activity to the same extent as SIK2 and SIK3 under basal conditions and in response to Fsk stimulation.

We performed immunohistochemical studies to evaluate effects of SIKs on the subcellular localization of the CRTCs (Fig. 1E & 1F). Under basal conditions, overexpressed CRTC2 displayed a nuclear or cytoplasmic/nuclear co-distribution in HEK293T cells coexpressing the catalytically inactive T175A SIK2 mutant. By contrast, overexpressed wild type SIK2 promoted CRTC2 accumulation almost exclusively in the cytoplasm. Fsk treatment inhibited the activity of coexpressed SIK2 and induced CRTC2 nuclear localization (Fig. 1E & 1F). Collectively, these results indicate that each of the SIKs regulates the subcellular localization and transcriptional activity of the CRTC family in a cAMP sensitive manner.

cAMP sensitivity of SIK3 and SIK1 depends upon two PKA sites that mediate 14-3-3 protein interaction

Although all three SIKs have been found to associate with 14-3-3 proteins, a potential role for cAMP/PKA in modulating this interaction has only been suggested for SIK2 and SIK3 [27, 28, 32, 33]. In addition, only SIK3's activity appears to be repressed by 14-3-3s *in vitro* [27]. Because PKA-mediated phosphorylation has been shown to interfere with the intracellular activity of SIKs, we systematically evaluated whether PKA regulates the activity of all three SIKs by controlling their association with 14-3-3s [10].

SIK3 is thought to contain three PKA phosphorylation sites that participate in 14-3-3 protein binding (Fig. 2A) [27]. However, only two PKA sites (T411 and S493) are conserved amongst vertebrates and invertebrates (Fig. 2B). Wild type (WT) and mutant SIK3 proteins carrying non-phosphorylatable (Ser/Ala) or phosphorylation mimic (Ser/Glu) substitutions repressed CRE reporter activity comparably under basal conditions (Fig. 2C). Fsk stimulated CRE reporter activity in cells expressing WT SIK3, but mutant SIK3 proteins containing Ala or Glu mutations at T411 and more potently at S493, blocked the stimulatory effects of Fsk (T411A/E = ~20–40% and S493A/E = ~13% CRE reporter activity upon Fsk treatment; Fig. 2C & 2D). By contrast, mutations in the non-conserved S568 site had no effect on CRE reporter activity in cells exposed to Fsk (SIK3 WT = ~90% and S568A/E = ~75–90% CRE reporter activity upon Fsk treatment). In keeping with these effects, cells expressing T411 and S493 phosphorylation-defective SIK3 proteins phosphorylated CRTC2/3 constitutively and were therefore resistant to inhibition by Fsk (Fig. 2E). To evaluate effects of PKA on the interaction of SIK3 with 14-3-3 proteins, we performed Co-IP experiments after Fsk

exposure (Fig. 2F). Mutations at T411 and S493 of SIK3 abolished 14-3-3 binding, while S568A had no effect. These results support the notion that PKA-mediated phosphorylation of SIK3 at T411 and S493 interferes with SIK3 catalytic activity by stimulating 14-3-3 protein binding.

Similar to SIK3, the predominantly nuclear SIK1 also contains two conserved PKA sites (Fig. 3A) [31, 34, 36]. Exposure to Fsk reversed the inhibitory effects of overexpressed SIK1 WT in the CRE reporter assay, but these effects were abrogated in cells expressing non-phosphorylatable PKA site mutations at T473 and S575 (Fig. 3B & 3C). Mutations at S575 in SIK1 were as potent in blocking stimulatory effects of Fsk as the PKA site double mutant (T473A/E = ~40% and S575A/E or T473A S575A = ~25% CRE reporter activity upon Fsk treatment). Indeed, the single S575A/E site mutants were as active as the T473A S575A double mutant in phosphorylating CRT2/3 even in cells exposed to Fsk (Fig. 3D). Nuclear SIK1 has been found to shuttle to the cytoplasm following its phosphorylation by PKA, a process that is blocked by mutation of S575 [31, 36]. In keeping with these results, epitope-tagged WT and S575A SIK1 proteins were both detected in the nucleus under basal conditions, and Fsk treatment promoted the cytoplasmic translocation of WT, but not S575A SIK1 (Fig. 3E & 3F). Similar to SIK3, 14-3-3 protein binding of SIK1 was dependent upon PKA site phosphorylation; Ala or Glu substitution at T473 and to a larger extent at S575, impaired the 14-3-3 association (Fig. 3G). These results indicate that S575 serves as the primary or “gatekeeper” 14-3-3 binding site in SIK1, modulating its activity as well as nucleocytoplasmic localization.

Collectively, the two PKA phosphorylation sites in SIK1 and SIK3 function as 14-3-3 binding sites, which mediate inhibitory effects of cAMP on their catalytic activity. Both kinases contain a dominant and a secondary 14-3-3 binding site that together presumably favor binding to dimeric 14-3-3 proteins.

Four PKA sites in SIK2 regulate catalytic activity and enable cooperative 14-3-3 protein binding

By contrast with the two sites in both SIK1 and SIK3, four PKA phosphorylation sites were identified in SIK2 that potentially effect 14-3-3 association (Fig. 4A) [7, 28, 29, 37]. Similar to studies with SIK1, Ser/Ala mutants at each PKA phospho-acceptor site blocked Fsk-induced CRE reporter activation in comparison to SIK2 WT (SIK2 WT = ~80% and PKA site mutants = ~6–35% CRE reporter activity upon Fsk treatment; Fig. 4B & 4C). Although conserved PKA site S587 (equivalent to S575 in SIK1) had the most pronounced effect on SIK2 activity as a single mutant, PKA site double mutants were more active than their corresponding single mutants (S358A T484A = ~6% and S358A S587A = ~4% CRE reporter activity upon Fsk treatment). Mutations at each of four individual PKA sites reduced the association of SIK2 with 14-3-3 proteins in Fsk-stimulated cells (Fig. 4D). Correspondingly, PKA site mutants were more active in phosphorylating CRT2/3 relative to SIK2 WT, with S587A being most potent. Similar to their effects in reporter assays, SIK2 mutants with Ala substitutions at two PKA sites (S358A S587A) exhibited lower 14-3-3 binding and enhanced kinase activity towards CRT2/3 relative to the respective single site mutants. Different PKA site double mutants in SIK2 have distinct effects on activity,

although the S358A S587A mutant was the most active in phosphorylating CRTC2/3 (Fig. 4E). Nevertheless, all SIK2 double-site mutants, including S358A S587A, were inhibited by Fsk, as revealed by the dephosphorylation of CRTC2/3 under these conditions. By contrast with double mutants, a triple PKA site mutant in SIK2 was fully resistant to cAMP inhibition (3A = S358A T484A S587A; Fig. 4F). The PKA site double mutants of SIK2 also differed in their interaction with 14-3-3s as well as with coexpressed CRTC3, with S358A S587A having lowest affinity for 14-3-3s and highest affinity for CRTC3 (Fig. 4G & 4H). Taken together, these results indicate that all four PKA-phosphorylation sites in SIK2 participate in catalytically inhibitory interactions with 14-3-3 proteins, although S587 exerts a dominant effect in this setting. Furthermore, the association of 14-3-3s with SIK2 appears to interfere with substrate binding.

The RK-region (595–624) is required for inhibition of SIK2 activity by 14-3-3 binding

The S575/S587 “gatekeeper” site is highly conserved between SIK1 and SIK2 with sequence homology expanding C-terminally into an RK-rich region consisting of interspersed basic and hydrophobic residues (hSIK1 = 583–612 with 9× Arg/Lys & 5× Leu; hSIK2 = 595–624 with 4× Arg/Lys & 6× Leu) (Fig. 5A) [31, 38]. The RK-rich region in SIK1 has been linked to cAMP responsiveness, because a SIK1 deletion mutant lacking these residues repressed CRE activity as effectively as a non-phosphorylatable proximal “gatekeeper” site (S575A) mutant [31]. To test the importance of SIK2’s RK-rich region for cAMP sensitivity and 14-3-3 binding, we generated a RK-rich region deletion (SIK2^{ΔRK}) as well as a SIK2 and SIK1 hybrid (SIK2-1), containing the RK-rich region and C-terminus of SIK1 (SIK2 C-terminally truncated after its last 14-3-3 site (S587); Fig. 5B). Protein amounts of overexpressed SIK2-1 were comparable to SIK1 and both kinases catalyzed the phosphorylation of CRTC2/3 and class IIA HDAC to the same extent (Fig. 5C). Exposure to Fsk strongly inhibited SIK2 WT and SIK2-1 activities, but Fsk effects on SIK2^{ΔRK} activity were relatively impaired even though the proximal PKA site at S587 is efficiently phosphorylated in this mutant. Moreover, exposure to Fsk still induced the association of SIK2^{ΔRK} with 14-3-3s, comparably to wild type SIK3 and SIK2 as well as SIK2-1 (Fig. 5D). Indeed, SIK2^{ΔRK} repressed CRE reporter activity more avidly than SIK2 WT following Fsk stimulation (SIK2 WT = ~60% and SIK2^{ΔRK} = ~25% CRE reporter activity upon Fsk treatment; Fig. 5E & 5F). In addition to its role in promoting cAMP sensitivity, the RK-rich region has also been shown to regulate nuclear localization of SIK1 [31]. Accordingly, the SIK2-1 hybrid containing the RK rich region from SIK1 was nuclear localized and shuttled to the cytoplasm in response to Fsk (Fig. 5G). Nevertheless, exposure to Fsk inhibited the activity of SIK2-1, which carries all four PKA/14-3-3 sites of SIK2, comparably to SIK2 in CRE reporter assays (Fig. 5H). These results suggest that the conserved RK-rich region is required for nuclear localization of SIK1, and for cAMP responsiveness of both SIK1 and SIK2.

***In vitro* SIK2 activity is modulated by 14-3-3 association and presence of the RK-rich region**

In previous studies, mutation of PKA sites in SIK2 did not appear to modulate its catalytic activity *in vitro* [28, 29]. Knowing the importance of 14-3-3 interactions in this setting, we purified FLAG-tagged versions of SIK2 WT, SIK2^{ΔRK}, and SIK2 AA (S358A S587A)

from HEK293T cells that had been exposed to Fsk (Fig. 6A). As expected, large quantities of 14-3-3 proteins were recovered from FLAG IPs of SIK2 WT and SIK2 RK, but amounts decreased for the non-phosphorylatable SIK2 AA mutant. To mimic an endogenous SIK2 substrate, we heterologously expressed and purified a CRTC2 fragment containing both regulatory SIK2 phosphorylation sites (S171 and S275, mCRTC2 147–297). Although WT and mutant SIK2 proteins were comparably phosphorylated by LKB1 at T175 within the activation loop, SIK2 RK and, to a greater extent, SIK2 AA were more active than wild type SIK2 in phosphorylating the CRTC2 fragment *in vitro* (Fig. 6B–D). Collectively, these results demonstrate that the PKA-dependent interaction of SIK2 with 14-3-3s is indeed critical for catalytic inhibition both intracellularly and by *in vitro* studies with the purified kinase.

Discussion

SIKs regulate CRTCs and class IIA HDACs by phosphorylating these proteins at sites that enhance 14-3-3 protein binding and cytoplasmic sequestration (Fig. 7A). We found that cAMP signaling inhibits the catalytic activity of all three SIK family members through PKA-induced 14-3-3 associations. As a result, CRTCs and HDACs undergo dephosphorylation and are liberated from 14-3-3s, allowing them to translocate to the nucleus. This molecular mechanism explains the responsiveness of CRTCs and class IIA HDACs to hormone-dependent changes in intracellular cAMP [10, 39].

SIKs contain multiple PKA/14-3-3 sites, which resemble the mode I consensus motif (RSXSXP; underlined = phosphorylated residue, and X = any residue) (Fig. 7B) [20]. With the exception of S343 in SIK2 (KSHRSS₃₄₃FPVEQ) all 14-3-3 sites in SIK family members have the consensus arginine at -3. SIK1 and SIK3 contain two PKA/14-3-3 sites and mutation of individual phospho-acceptor sites abolished the 14-3-3 association and rendered kinase activity insensitive to cAMP. In contrast, SIK2 has four PKA phosphorylation sites, which exhibit cooperativity in binding to 14-3-3s. Since 14-3-3 proteins bind to ligands as dimers, they could associate with SIK2 in multiple ways [21, 22]. Consistent with this notion, PKA/14-3-3 site double mutants remain cAMP sensitive, but mutation of three PKA sites renders SIK2 fully resistant to cAMP [29].

In general, PKA site mutants have no effect on LKB1-mediated phosphorylation of the SIK activation loop, arguing against an effect of PKA-mediated phosphorylation or 14-3-3s on intrinsic catalytic activity of these kinases [1, 28, 29]. Our results rather favor an indirect mechanism by which binding of 14-3-3 dimers causes conformational changes that inhibit SIK catalytic activity. Such structural alterations have been reported for other 14-3-3 ligands including nitrate reductase (NR), RAF proto-oncogene serine/threonine-protein kinase (RAF1), and M-phase inducer phosphatase 2 (CDC25B) [23, 40, 41]. In case of CDC25B, repression of phosphatase activity is thought to be dependent upon 14-3-3 dimers that form an intramolecular bridge between weak 14-3-3 sites inside the N-terminus (S151 or S230) together with the dominant S323 site, blocking cyclin/CDK substrate access as well as impairing access to the nucleus [23, 42]. The PKA/14-3-3 sites of the three SIKs are located distal to the N-terminal kinase domain, indicating that dimeric 14-3-3 association might cause a conformational rearrangement within the SIKs that physically excludes CRTC and

HDAC binding. Consistent with this model, double PKA/14-3-3 mutants of SIK2 exhibit increased CRT3 substrate association.

Binding of 14-3-3s to serotonin N-acetyltransferase (AANAT), which is also PKA-dependent, revealed extensive molecular interactions outside of the AANAT 14-3-3 binding site [24, 43]. Similarly, the RK-rich region (595–624) of SIK2 may participate in the PKA/14-3-3-dependent conformational rearrangement, because its deletion uncouples 14-3-3 binding from the subsequent impairment in SIK2 activity. Full cAMP/PKA sensitivity was restored with a hybrid protein carrying the RK-rich region and C-terminus of SIK1, similar to previously described SIK1/ SIK2 chimeras with interchanged RK-rich regions (~30 residues) [31]. These results suggest that the RK-rich region fulfills a conserved role for PKA/14-3-3-mediated inhibition between SIK1 and SIK2.

In addition to the SIKs, the MAP/microtubule affinity-regulating kinases (MARKs) subfamily of AMPK related Ser/Thr kinases has also been shown to interact with 14-3-3 proteins [32, 44]. Although MARKs have been primarily linked to the regulation of cell polarity, they can also phosphorylate CRTCs and class IIA HDACs [13, 14, 45, 46]. However, the association of 14-3-3s with MARKs is insensitive to cAMP and at least partially regulated by atypical PKC [14, 44, 47]. In contrast to the SIKs, the association of 14-3-3s with MARKs apparently modulates their plasma membrane localization but not their catalytic activity [44]. Future *in vitro* studies with purified recombinant proteins should provide insight into the mechanisms by which 14-3-3s modulate SIK and MARK activities.

Material and Methods

Sections of the methods were previously described and are reprinted here, partly verbatim, for reference [14].

Small Molecules

Small molecules were solubilized in DMSO (ACS, Sigma-Aldrich) at the indicated concentrations and stored until usage at -80°C (long term storage) or -20°C (working dilution): 20 mM Forskolin (Sigma-Aldrich) and 2 mM Carfilzomib (PR-171) (Selleck Chemicals).

Antibodies

The antibodies used in this study were purchased from Santa Cruz Biotechnology (14-3-3 ϵ polyclonal), EMD Millipore (α -tubulin), Sigma-Aldrich (FLAG M2), Covance (GFP), Roche (Anti-HA-Peroxidase), Qiagen (Penta-His), MRC Protein Phosphorylation and Ubiquitylation Unit (P-SIK2 T175), and Cell Signaling Technology (14-3-3[pan], P-CREB S133, P-CRTC2 S171, HA [C29F4], P-HDAC4(5/7) S246, P-HDAC4(5/7) S632, P-PKA substrate, P-VASP S157, SIK2). The P-CRTC3 S273 antiserum was previously described [14].

See Antiserum Production for the P-SIK1 S575 antiserum (PBL #7404).

Antiserum Production

All animal procedures were approved by the Institutional Animal Care and Use Committee of the Salk Institute and were conducted in accordance with the PHS Policy on Humane Care and Use of Laboratory Animals (PHS Policy, 2015), the U.S. Government Principles for Utilization and Care of Vertebrate Animals Used in Testing, Research and Training, the NRC Guide for Care and Use of Laboratory Animals (8th edition) and the USDA Animal Welfare Act and Regulations. Three 10 to 12-week old, female New Zealand white rabbits, weighing 3.0 to 3.2 kg at beginning of the study, were procured from Irish Farms (I.F.P.S. Inc., Norco, California, USA). All animals were housed in an AAALAC accredited facility in a climate controlled environment (65–72 degrees Fahrenheit, 30–70% humidity) under 12-hour light/12-hour dark cycles. Rabbits were provided with ad libitum feed (5326 Lab Diet High Fiber), micro-filtered water and weekly fruits, vegetables and alfalfa hay for enrichment. Upon arrival, animals were physically examined by veterinary staff for good health and acclimated for two weeks prior to initiation of antiserum production. Each animal was monitored daily by the veterinary staff for signs of complications and weighed every two weeks. Routine physical exams were also performed by the veterinarian quarterly on all rabbits.

Three rabbits were injected with a peptide fragment encoding pSer⁵⁷⁵Cys⁵⁸⁹ human SIK1(566–589)-NH₂ coupled to keyhole limpet hemocyanin via maleimide. The peptide, VSFQEGRRR(pS)DTSLTQGLKAFRQC-NH₂, was synthesized and purified by RS Synthesis. The antigen was delivered to host animals using multiple intradermal injections of peptide-KLH conjugate in Complete Freund's Adjuvant (initial inoculation) or incomplete Freund's adjuvant (booster inoculations) every three weeks. Rabbits were bled, <10% total blood volume, one week following booster injections and bleeds screened for titer and specificity. Animals were administered 1–2 mg/kg Acepromazine IM prior to injections of antigen or blood withdrawal. At the termination of study, animals were exsanguinated under anesthesia (ketamine 50 mg/kg and acepromazine 1 mg/kg, IM) and euthanized with an overdose of pentobarbital sodium and phenytoin sodium (1 ml/4.5 kg of body weight IC to effect). After blood was collected death was confirmed. All animal procedures were conducted by experienced veterinary technicians, under the supervision of Salk Institute veterinarians.

The phospho-SIK1 S575 antiserum obtained from the rabbit (code PBL #7404) with the best characteristics of titer and specificity was used for all experiments. To ensure that the same batch of serum could be used for this and future studies, a large volume of serum (18 ml) from two bleeds with similar profiles was depleted of antibodies recognizing the non-phosphorylated form of SIK1 by passing over a column containing Cys⁵⁸⁹ hSIK1(566–589)-NH₂-agarose resin. Covalent attachment of the peptide to resin (Sulfolink coupling resin, Thermo Fisher) was per manufacturer's instructions.

Plasmids

For overexpression studies plasmids were used that contained the *Homo sapiens* Ubiquitin C promoter (pUbc), whose activity is unaffected by cAMP signaling. The plasmids -

pUbC-3xFLAG-TEVsite-His₆-MCS-IRES-eGFP and pUbC-3xHA-MCS - have been described previously (MCS = multiple cloning site) [14].

The cDNAs (h = *H. sapiens*, m = *Mus musculus*) for overexpression constructs originated from the Plasmid Information Database (PlasmID; hSIK1 and hSIK3) and Clontech (EGFP) or were previously generated [14]. The plasmids code for the following proteins (UniProt identifier): mCRTC1 (Q68ED7-1), mCRTC2 (Q3U182-1), mCRTC3 (Q91X84-1), hSIK1 (P57059-1), mSIK2 (Q8CFH6-1), hSIK3 (Q9Y2K2-1).

The hSIK1 containing plasmid was cloned by restriction enzyme digest, the hSIK3 plasmid by fusion PCR (deletion of an internal segment), the SIK2 RK plasmid by inverse PCR (mSIK2 596–622), and the SIK2-1 plasmid by fusion PCR (mSIK2 2–595 fused with hSIK1 583–783). Fusion PCR was performed as previously described [48]. All phospho-acceptor mutations were introduced via single or cumulative site-directed mutagenesis.

The *Escherichia coli* expression plasmid of mCRTC2(147–297) was generated by cloning the corresponding codon optimized fragment (generated by Biomatik Corporation) into a derivative of pET22b (Novagen [EMD Millipore]) coding for STII-Trx-TEVsite-MCS-His₆ (STII = Strep-Tag II; MCS = multiple cloning site).

Cell Culture

HEK293T cells were purchased from ATCC (CRL-11268) and propagated in DMEM media (Gibco®, high glucose) supplemented with 10% Fetal Bovine Serum (Gemini Bio-Products) and 100 U/ml penicillin-streptomycin (Corning Inc.).

Overexpression & Immunoprecipitation (IP)

Experiments were performed in 6 well plates by reverse transfecting HEK293T cells (2.5×10^6 cells) with 2 µg plasmid DNA using Lipofectamine® 2000 (Invitrogen). 48 h post transfection cells were collected in PBS and resuspended in lysis buffer (50 mM Tris, 150 mM NaCl, 10% glycerol, 1% Igepal [Sigma-Aldrich], 1 mM DTT, EDTA-free cOmplete™ Protease Inhibitor Cocktail [Roche], Phosphatase Inhibitor Cocktail 2 and 3 [Sigma-Aldrich], 1 µM Carfilzomib; pH 8.0). The supernatant (= cell lysate) was either used in IP experiments or directly mixed with SDS-PAGE loading buffer. In all IP experiments, cells were pre-treated for 1 h with 1 µM Carfilzomib prior to cell lysis. Cell lysates were incubated with anti-FLAG® M2 magnetic beads and 3xFLAG peptide (100 µg/ml final) was used to elute bound proteins (both Sigma-Aldrich).

Immunofluorescence

HEK293T cells (0.75×10^6 cells) were plated in Poly-D-Lysine coated glass bottom dishes (MatTek Corporation) and reverse transfected with Lipofectamine® 2000 (Invitrogen) using 1 µg of plasmid DNA (total): hSIK1, SIK2-1 hybrid, mSIK2 (all pUbC-3xFLAG backbone), and mCRTC2 (pUbC-3xHA backbone). 24 h post-transfection cells were treated with either DMSO or 10 µM Forskolin for 30 min. Cells were fixed with 4% paraformaldehyde and incubated with primary antibodies (FLAG M2, HA [C29F4]). Samples were incubated with secondary antibodies conjugated with Alexa Fluor® - 568 (goat anti-mouse) or in case of

FLAG/HA co-staining Alexa Fluor® - 568 and - 647 (goat anti-mouse & goat anti-rabbit) (Life Technologies). Counterstaining with DAPI (Cayman Chemical Company) was performed before image acquisition (LSM 710; Carl Zeiss).

Luciferase Reporter Assays

Luciferase reporter assays were performed in 96 well plates by reverse transfecting HEK293T cells (100,000 cells). For each well 80 ng of DNA was used: 10 ng of EVX-Luc reporter plasmid (2× CRE half-sites, firefly luciferase) [14], 10 ng of FLAG-tagged CRTC1–3 plasmids, 20 ng of FLAG-tagged SIK plasmids, 40 ng of empty pUbC plasmid. 24 h post transfection 10 μM Forskolin was added and cells further incubated for 4 h. DMSO served as the control treatment (each well 1% DMSO final). Next, 10 μl of Bright-Glo™ (Promega) was added per well and luciferase activity measured in a GloMax® multi microplate reader (Promega). All reporter assays were at least repeated twice and representative data is shown.

SIK2 Kinase Assay

Expression and Ni-NTA purification of STII-Trx-TEVsite-mCRTC2(147–297)-His₆ was performed as previously described [49]. Differing from the protocol an expression scale of 600 ml LB medium and buffers containing 1M NaCl were used. Following purification, the protein was dialyzed into storage buffer (50 mM Tris, 150 mM NaCl, 10% glycerol; pH 8.0) using a Slide-A-Lyzer™ MINI device (Thermo Fisher Scientific Inc.), concentrated using Amicon® Ultra (EMD Millipore) (440 μM final), flash frozen in liquid nitrogen, and stored at –80 °C.

SIK2 protein purification [SIK2 wild type, SIK2^{RK}, and SIK2^{S358A S587A}] was performed in 4 × 100 mm dishes by reverse transfecting HEK293T cells (1.5 × 10⁷ cells) with 12 μg plasmid DNA using Lipofectamine® 2000 (Invitrogen). 48 h post transfection cells were treated for 1h with 1 μM Carfilzomib and 10 μM Forskolin. Cell lysis was performed as described in the IP protocol. Following lysate incubation anti-FLAG® M2 magnetic beads were washed once in lysis buffer (50 mM Tris, 150 mM NaCl, 10% glycerol, 1% Igepal [Sigma-Aldrich], 1 mM DTT, EDTA-free cOmplete™ Protease Inhibitor Cocktail [Roche], Phosphatase Inhibitor Cocktail 2 and 3 [Sigma-Aldrich], 1 μM Carfilzomib; pH 8.0) and two times in buffer lacking the detergent Igepal. The identical buffer was used for elution after addition of 3xFLAG peptide (100 μg/ml final). Aliquots of SIK2 proteins were flash frozen in liquid nitrogen and stored at –80 °C until usage. SIK2 protein concentration was determined after SDS-PAGE and Coomassie Brilliant Blue staining (Thermo Fisher Scientific Inc.) by comparing the respective band intensities to reference bands (proteins of known concentration). Final SIK2 concentrations were estimated to be between 0.8 – 1.1 μM.

The SIK2 kinase assays were performed in assay buffer (50 mM Tris, 10 mM MgCl₂; pH 7.5) at an overall volume of 80 μl. mCRTC2(147–297) protein was diluted in assay buffer to 80 μM. To start the reaction components were sequentially added to pre-chilled assay buffer (incubation on ice): 1 μl of mCRTC2(147–297) (1 μM final), 0.8 μl of 10 mM ATP solution (10 μM final; Sigma-Aldrich), and ~4–5 μl SIK2 proteins (0.05 μM final). The reaction tubes were vortexed, spun down, and incubated at 30 °C in a ThermoMixer® R (Eppendorf AG).

At the indicated time points 10 μ l of the reaction mixture was removed and boiled after addition of SDS sample buffer (supplemented with 10 mM EDTA).

Sequence Alignment

Amino acid sequences were aligned using MegAlign and Clustal W method (DNASTAR v7).

Statistical Analysis

Data are either presented as the mean \pm SEM. or \pm SD. Statistical analysis was performed using Microsoft Excel (Microsoft Corporation) and graphical presentations were generated using SigmaPlot (Systat Software Inc.) or PRISM (GraphPad).

Acknowledgments

This work was supported by NIH grant R01 DK083834, the Leona M. and Harry B. Helmsley Charitable Trust, the Clayton Foundation for Medical Research, and the Kieckhefer Foundation.

Abbreviations

AMPK	AMP-activated protein kinase
CRTC	cAMP-regulated transcriptional coactivator
CRE	cAMP-response element
CREB	cAMP response-element binding protein
Fsk	Forskolin
HDAC	histone deacetylase
IP	immunoprecipitation
PKA	protein kinase A
SIK	salt-inducible kinase

References

1. Lizcano JM, et al. LKB1 is a master kinase that activates 13 kinases of the AMPK subfamily, including MARK/PAR-1. *EMBO J.* 2004; 23(4):833–43. [PubMed: 14976552]
2. Shackelford DB, Shaw RJ. The LKB1-AMPK pathway: metabolism and growth control in tumour suppression. *Nat Rev Cancer.* 2009; 9(8):563–75. [PubMed: 19629071]
3. Berdeaux R, et al. SIK1 is a class II HDAC kinase that promotes survival of skeletal myocytes. *Nat Med.* 2007; 13(5):597–603. [PubMed: 17468767]
4. Dentin R, et al. Insulin modulates gluconeogenesis by inhibition of the coactivator TORC2. *Nature.* 2007; 449(7160):366–9. [PubMed: 17805301]
5. Funato H, et al. Forward-genetics analysis of sleep in randomly mutagenized mice. *Nature.* 2016; 539(7629):378–383. [PubMed: 27806374]
6. Sanosaka M, et al. Salt-inducible kinase 3 deficiency exacerbates lipopolysaccharide-induced endotoxin shock accompanied by increased levels of pro-inflammatory molecules in mice. *Immunology.* 2015; 145(2):268–78. [PubMed: 25619259]

7. Sreaton RA, et al. The CREB coactivator TORC2 functions as a calcium- and cAMP-sensitive coincidence detector. *Cell*. 2004; 119(1):61–74. [PubMed: 15454081]
8. Wein MN, et al. SIKs control osteocyte responses to parathyroid hormone. *Nat Commun*. 2016; 7:13176. [PubMed: 27759007]
9. Shaw RJ, et al. The kinase LKB1 mediates glucose homeostasis in liver and therapeutic effects of metformin. *Science*. 2005; 310(5754):1642–6. [PubMed: 16308421]
10. Altarejos JY, Montminy M. CREB and the CRTC co-activators: sensors for hormonal and metabolic signals. *Nat Rev Mol Cell Biol*. 2011; 12(3):141–51. [PubMed: 21346730]
11. Walkinshaw DR, et al. The tumor suppressor kinase LKB1 activates the downstream kinases SIK2 and SIK3 to stimulate nuclear export of class IIa histone deacetylases. *J Biol Chem*. 2013; 288(13):9345–62. [PubMed: 23393134]
12. Henriksson E, et al. SIK2 regulates CRTCs, HDAC4 and glucose uptake in adipocytes. *J Cell Sci*. 2015; 128(3):472–86. [PubMed: 25472719]
13. Jansson D, et al. Glucose controls CREB activity in islet cells via regulated phosphorylation of TORC2. *Proc Natl Acad Sci U S A*. 2008; 105(29):10161–6. [PubMed: 18626018]
14. Sonntag T, et al. Analysis of a cAMP regulated coactivator family reveals an alternative phosphorylation motif for AMPK family members. *PLoS One*. 2017; 12(2):e0173013. [PubMed: 28235073]
15. Clark K, et al. Phosphorylation of CRTC3 by the salt-inducible kinases controls the interconversion of classically activated and regulatory macrophages. *Proc Natl Acad Sci U S A*. 2012; 109(42):16986–91. [PubMed: 23033494]
16. Kozhemyakina E, et al. Parathyroid hormone-related peptide represses chondrocyte hypertrophy through a protein phosphatase 2A/histone deacetylase 4/MEF2 pathway. *Mol Cell Biol*. 2009; 29(21):5751–62. [PubMed: 19704004]
17. Gardino AK, Smerdon SJ, Yaffe MB. Structural determinants of 14-3-3 binding specificities and regulation of subcellular localization of 14-3-3-ligand complexes: a comparison of the X-ray crystal structures of all human 14-3-3 isoforms. *Semin Cancer Biol*. 2006; 16(3):173–82. [PubMed: 16678437]
18. Martens GJ, Piosik PA, Danen EH. Evolutionary conservation of the 14-3-3 protein. *Biochem Biophys Res Commun*. 1992; 184(3):1456–9. [PubMed: 1375463]
19. Yang X, et al. Structural basis for protein-protein interactions in the 14-3-3 protein family. *Proc Natl Acad Sci U S A*. 2006; 103(46):17237–42. [PubMed: 17085597]
20. Fu H, Subramanian RR, Masters SC. 14-3-3 proteins: structure, function, and regulation. *Annu Rev Pharmacol Toxicol*. 2000; 40:617–47. [PubMed: 10836149]
21. Yaffe MB. How do 14-3-3 proteins work?-- Gatekeeper phosphorylation and the molecular anvil hypothesis. *FEBS Lett*. 2002; 513(1):53–7. [PubMed: 11911880]
22. Yaffe MB, et al. The structural basis for 14-3-3:phosphopeptide binding specificity. *Cell*. 1997; 91(7):961–71. [PubMed: 9428519]
23. Giles N, Forrest A, Gabrielli B. 14-3-3 acts as an intramolecular bridge to regulate cdc25B localization and activity. *J Biol Chem*. 2003; 278(31):28580–7. [PubMed: 12764136]
24. Obsil T, et al. Crystal structure of the 14-3-3zeta:serotonin N-acetyltransferase complex. a role for scaffolding in enzyme regulation. *Cell*. 2001; 105(2):257–67. [PubMed: 11336675]
25. Taylor SS, et al. Assembly of allosteric macromolecular switches: lessons from PKA. *Nat Rev Mol Cell Biol*. 2012; 13(10):646–58. [PubMed: 22992589]
26. Mayr B, Montminy M. Transcriptional regulation by the phosphorylation-dependent factor CREB. *Nat Rev Mol Cell Biol*. 2001; 2(8):599–609. [PubMed: 11483993]
27. Berggreen C, et al. cAMP-elevation mediated by beta-adrenergic stimulation inhibits salt-inducible kinase (SIK) 3 activity in adipocytes. *Cell Signal*. 2012; 24(9):1863–71. [PubMed: 22588126]
28. Henriksson E, et al. The AMPK-related kinase SIK2 is regulated by cAMP via phosphorylation at Ser358 in adipocytes. *Biochem J*. 2012; 444(3):503–14. [PubMed: 22462548]
29. Patel K, et al. The LKB1-salt-inducible kinase pathway functions as a key gluconeogenic suppressor in the liver. *Nat Commun*. 2014; 5:4535. [PubMed: 25088745]

30. Katoh Y, et al. Silencing the constitutive active transcription factor CREB by the LKB1-SIK signaling cascade. *FEBS J.* 2006; 273(12):2730–48. [PubMed: 16817901]
31. Katoh Y, et al. Salt-inducible kinase-1 represses cAMP response element-binding protein activity both in the nucleus and in the cytoplasm. *Eur J Biochem.* 2004; 271(21):4307–19. [PubMed: 15511237]
32. Al-Hakim AK, et al. 14-3-3 cooperates with LKB1 to regulate the activity and localization of QSK and SIK. *J Cell Sci.* 2005; 118(Pt 23):5661–73. [PubMed: 16306228]
33. Hashimoto YK, et al. Importance of autophosphorylation at Ser186 in the A-loop of salt inducible kinase 1 for its sustained kinase activity. *J Cell Biochem.* 2008; 104(5):1724–39. [PubMed: 18348280]
34. Stewart R, et al. Regulation of SIK1 abundance and stability is critical for myogenesis. *Proc Natl Acad Sci U S A.* 2013; 110(1):117–22. [PubMed: 23256157]
35. Conkright MD, et al. TORCs: transducers of regulated CREB activity. *Mol Cell.* 2003; 12(2):413–23. [PubMed: 14536081]
36. Takemori H, et al. ACTH-induced nucleocytoplasmic translocation of salt-inducible kinase. Implication in the protein kinase A-activated gene transcription in mouse adrenocortical tumor cells. *J Biol Chem.* 2002; 277(44):42334–43. [PubMed: 12200423]
37. MacKenzie KF, et al. PGE(2) induces macrophage IL-10 production and a regulatory-like phenotype via a protein kinase A-SIK-CRTC3 pathway. *J Immunol.* 2013; 190(2):565–77. [PubMed: 23241891]
38. Berdeaux R. Metabolic regulation by salt inducible kinases. *Front Biol (Beijing).* 2011; 6(3):231–241.
39. Mihaylova MM, et al. Class IIa histone deacetylases are hormone-activated regulators of FOXO and mammalian glucose homeostasis. *Cell.* 2011; 145(4):607–21. [PubMed: 21565617]
40. Lambeck IC, et al. Molecular mechanism of 14-3-3 protein-mediated inhibition of plant nitrate reductase. *J Biol Chem.* 2012; 287(7):4562–71. [PubMed: 22170050]
41. Fischer A, et al. Regulation of RAF activity by 14-3-3 proteins: RAF kinases associate functionally with both homo- and heterodimeric forms of 14-3-3 proteins. *J Biol Chem.* 2009; 284(5):3183–94. [PubMed: 19049963]
42. Forrest A, Gabrielli B. Cdc25B activity is regulated by 14-3-3. *Oncogene.* 2001; 20(32):4393–401. [PubMed: 11466620]
43. Ganguly S, et al. Melatonin synthesis: 14-3-3-dependent activation and inhibition of arylalkylamine N-acetyltransferase mediated by phosphoserine-205. *Proc Natl Acad Sci U S A.* 2005; 102(4):1222–7. [PubMed: 15644438]
44. Goransson O, et al. Regulation of the polarity kinases PAR-1/MARK by 14-3-3 interaction and phosphorylation. *J Cell Sci.* 2006; 119(Pt 19):4059–70. [PubMed: 16968750]
45. Chang S, et al. An expression screen reveals modulators of class II histone deacetylase phosphorylation. *Proc Natl Acad Sci U S A.* 2005; 102(23):8120–5. [PubMed: 15923258]
46. Drewes G, et al. MARK, a novel family of protein kinases that phosphorylate microtubule-associated proteins and trigger microtubule disruption. *Cell.* 1997; 89(2):297–308. [PubMed: 9108484]
47. Kusakabe M, Nishida E. The polarity-inducing kinase Par-1 controls *Xenopus* gastrulation in cooperation with 14-3-3 and aPKC. *EMBO J.* 2004; 23(21):4190–201. [PubMed: 15343271]
48. Sonntag T, Mootz HD. An intein-cassette integration approach used for the generation of a split TEV protease activated by conditional protein splicing. *Mol Biosyst.* 2011; 7(6):2031–9. [PubMed: 21487580]
49. Zettler J, et al. SPLICEFINDER - a fast and easy screening method for active protein trans-splicing positions. *PLoS One.* 2013; 8(9):e72925. [PubMed: 24023792]
50. The UniProt Consortium. UniProt: the universal protein knowledgebase. *Nucleic Acids Res.* 2017; 45(D1):D158–D169. [PubMed: 27899622]

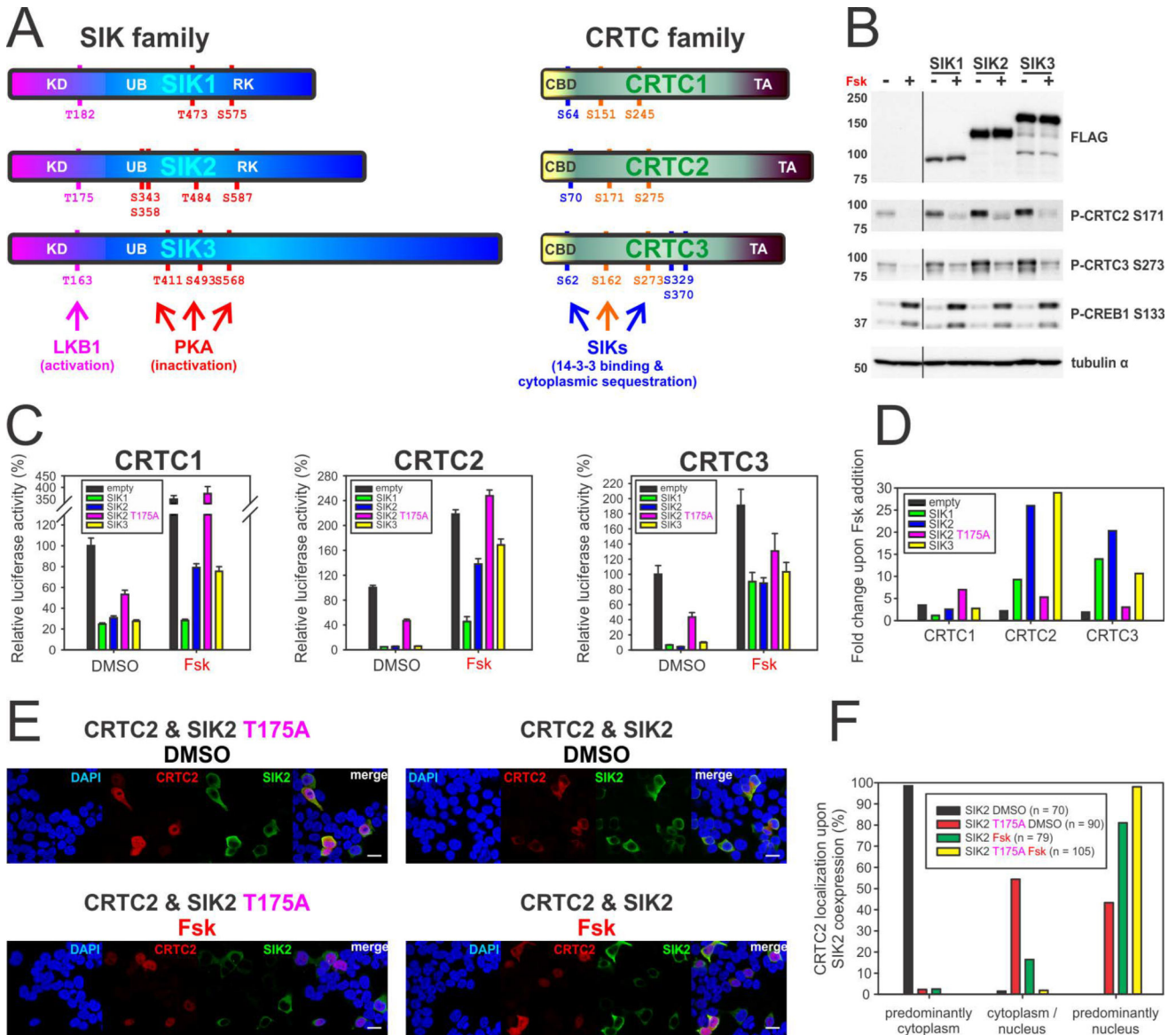


Fig. 1. SIK family members are regulated by cAMP signaling

A) To scale representation of the salt-inducible kinase (SIK) and the cAMP-regulated transcriptional coactivator (CRTC) protein families (according to *Homo sapiens* SIKs and *Mus musculus* CRTCs proteins). SIK activity requires activation loop phosphorylation inside the kinase domain (KD) by STK11/LKB1 (pink). The interaction of SIKs with LKB1 is facilitated by the conserved ubiquitin-associated domain (UB). All SIKs are subject to PKA-mediated phosphorylation which is thought to impair their activity (red). The RK-rich region (RK) represents a conserved domain among SIK1 & SIK2, facilitating nuclear translocation of SIK1. CRTC members contain multiple SIK phosphorylation sites that mediate cytoplasmic sequestration upon 14-3-3 interaction (blue & orange). Two of those conserved sites function cooperatively among all CRTCs (orange: S171 and S275 in CRTC2; CBD = CREB binding domain, TA = transactivation domain) B) Western blot analysis of the overexpression of FLAG-tagged SIK family members. In HEK293T cells the P-CRTC3

S273 antibody recognizes two bands, the upper band being CRTC2 and the lower band CRTC3 (calculated molecular weight: ~ 73 and 67 kDa); while the upper band of the P-CREB S133 antibody corresponds to CREB1 and the lower band to ATF1 (calculated molecular weight: ~ 37 and 29 kDa). (DMSO/Fsk treatment for 1h) C) EVX-Luc reporter assay measuring the effect of SIK1–3 upon the transcriptional activity of coexpressed CRTC1–3. EVX-Luc activity was measured after 4 h of DMSO/Fsk treatment. (n = 5/10, ± SEM) D) Graph depicting the corresponding fold changes in reporter activity upon Fsk treatment. E) Immunofluorescence of HEK293T cells co-transfected with FLAG-tagged SIK2 (wild type and T175A) and HA-tagged CRTC2. Cells were co-stained for FLAG & HA epitopes and counterstained with DAPI. (DMSO/Fsk treatment for 30 min; scale bar indicates 20 µm) F) Graph depicting the relative localization of CRTC2 upon SIK2 coexpression as well as upon Fsk treatment.

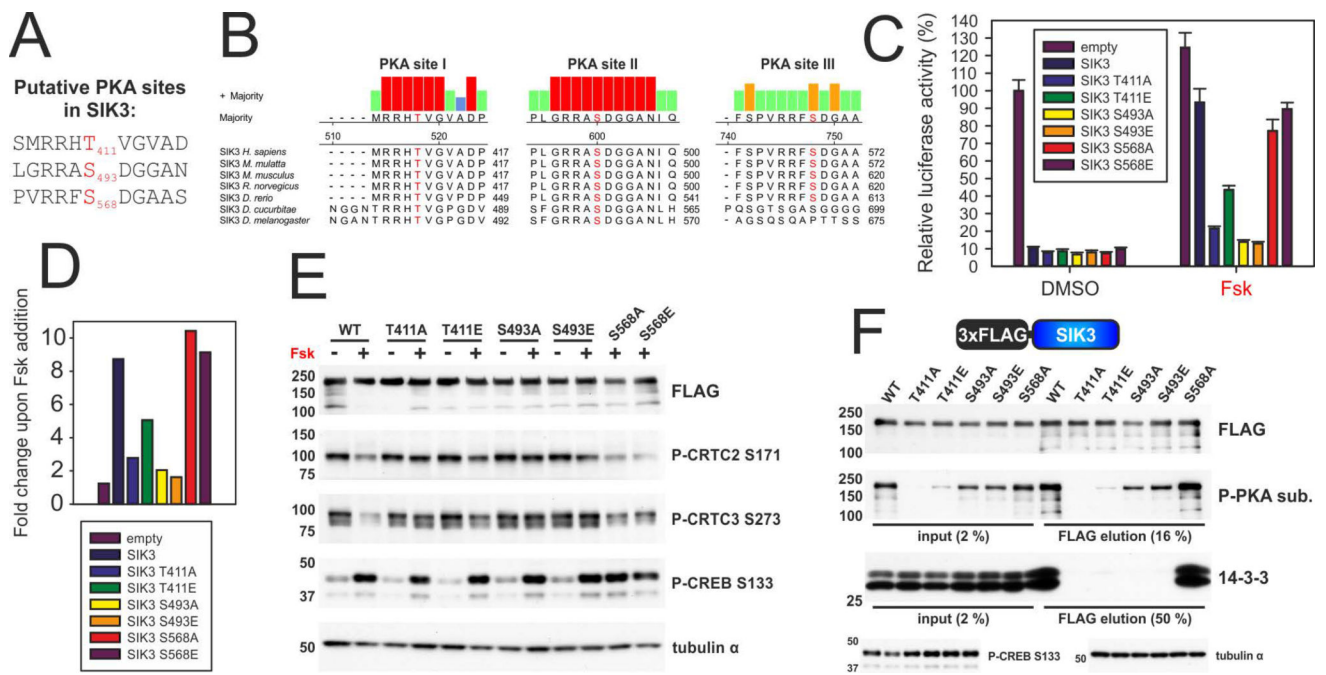


Fig. 2. SIK3 activity and 14-3-3 binding

A) Primary sequences of putative PKA sites in *H. sapiens* / *M. musculus* SIK3 (*H. sapiens* numbering). Phosphorylated residues are shown in red. B) Sequence alignment of SIK3 proteins from vertebrate and invertebrate species (obtained via UniProt [50]). Depicted regions are PKA sites I–III, out of which I and II are conserved (corresponding to T411 and S493 in *H. sapiens*). Phosphorylated Thr/Ser are highlighted in red. C) EVX-Luc reporter assay measuring the effect of SIK3 PKA site mutants upon the transcriptional activity of coexpressed CRTC3. EVX-Luc activity was measured after 4 h of DMSO/Fsk treatment. (n = 5, \pm SEM) D) Graph depicting the corresponding fold changes in reporter activity upon Fsk treatment. E) Western blot analysis showing the effects of overexpressed FLAG-tagged SIK3 wild type (WT) and PKA site mutants on CRTC phosphorylation. (DMSO/Fsk treatment for 1h) F) Western blot analysis of the Co-IP of FLAG-tagged SIK3 PKA site mutants with endogenous 14-3-3 proteins. (Fsk treatment for 1h)

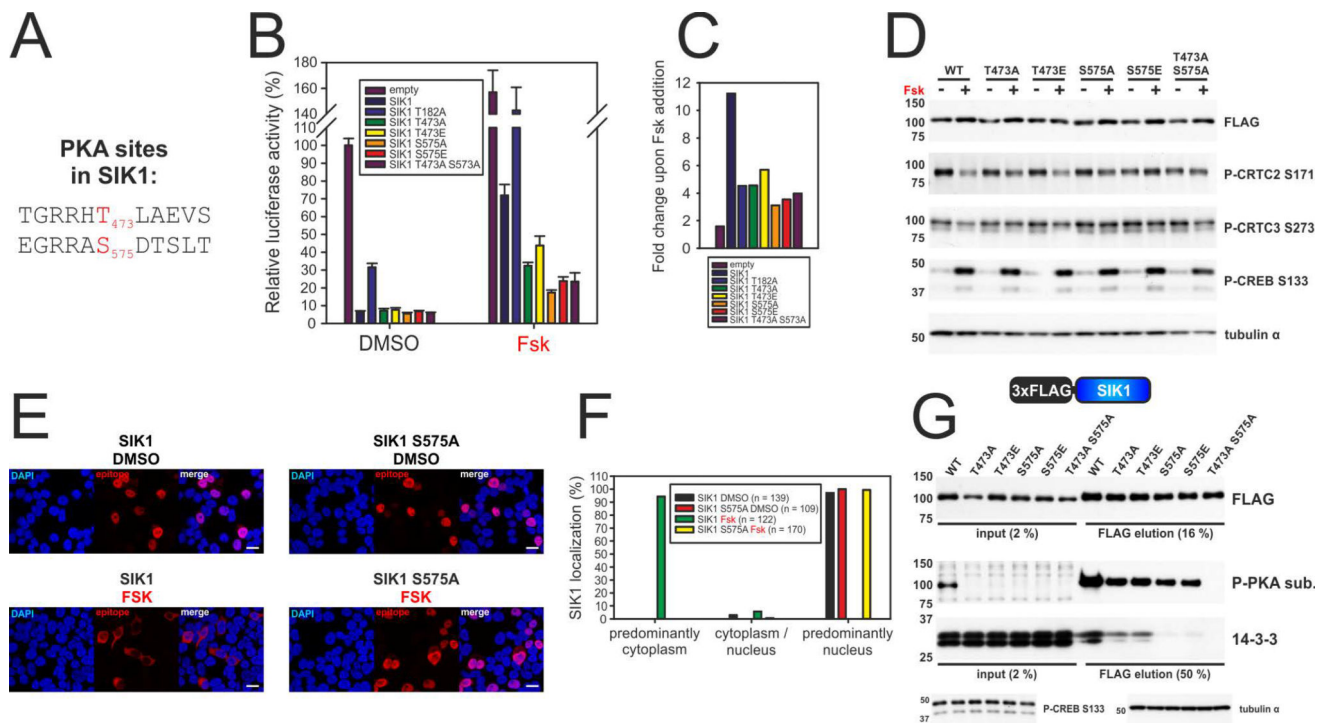


Fig. 3. SIK1 activity, nuclear localization, and 14-3-3 binding

A) Primary sequences of PKA sites in *H. sapiens* / *M. musculus* SIK1 (*H. sapiens* numbering). Phosphorylated residues are shown in red. B) EVX-Luc reporter assay measuring the effect of SIK1 PKA site mutants upon the transcriptional activity of coexpressed CRTC3. EVX-Luc activity was measured after 4 h of DMSO/Fsk treatment. (n = 5, ± SEM) C) Graph depicting the corresponding fold changes in reporter activity upon Fsk treatment. D) Western blot analysis showing the effects of overexpressed FLAG-tagged SIK1 wild type (WT) and PKA site mutants on CRTC phosphorylation. (DMSO/Fsk treatment for 1h) E) Immunofluorescence of HEK293T cells transfected with FLAG-tagged SIK1 (wild type and S575A). Cells were stained for FLAG epitope and counterstained with DAPI. (DMSO/Fsk treatment for 30 min; scale bar indicates 20 μm) F) Graph depicting the relative subcellular localization of SIK1 upon Fsk treatment. G) Western blot analysis of the Co-IP of FLAG-tagged SIK1 PKA site mutants with endogenous 14-3-3 proteins. (Fsk treatment for 1h)

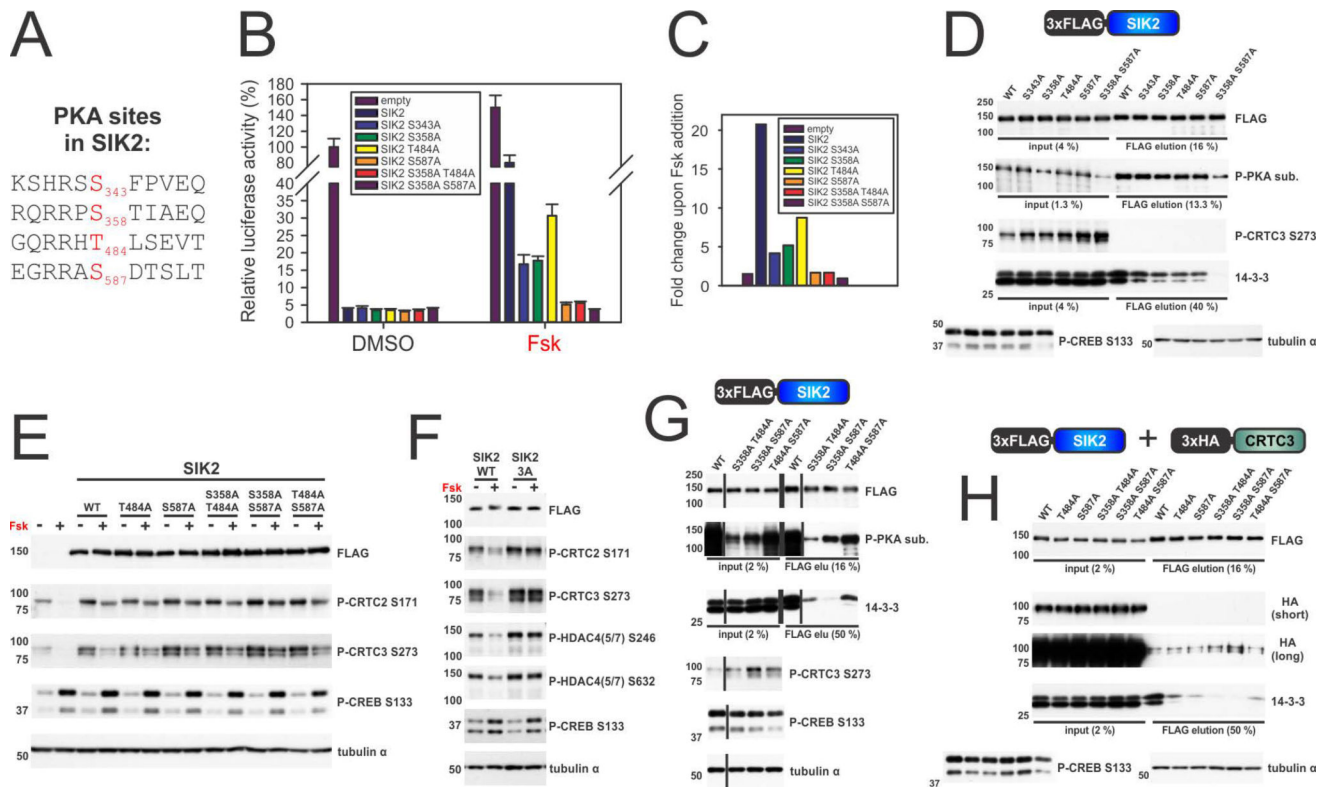


Fig. 4. Cooperative 14-3-3 binding of SIK2

A) Primary sequences of PKA sites in *H. sapiens* / *M. musculus* SIK2. Phosphorylated residues are shown in red. B) EVX-Luc reporter assay measuring the effect of SIK2 PKA site mutants upon the transcriptional activity of coexpressed CRT3. EVX-Luc activity was measured after 4 h of DMSO/Fsk treatment. (n = 5, ± SEM) C) Graph depicting the corresponding fold changes in reporter activity upon Fsk treatment. D) Western blot analysis of the Co-IP of FLAG-tagged SIK2 PKA site mutants with endogenous 14-3-3 proteins. (Fsk treatment for 1h) E) & F) Western blot analysis showing the effects of overexpressed FLAG-tagged SIK2 wild type (WT) and PKA site mutants on CRTC and class IIA HDAC phosphorylation (3A = S358A T484A S587A). (DMSO/Fsk treatment for 1h) G) Western blot analysis of the Co-IP of FLAG-tagged SIK2 PKA site double mutants with endogenous 14-3-3 proteins. (Fsk treatment for 1h) H) Western blot analysis of the Co-IP of FLAG-tagged SIK2 PKA site mutants with coexpressed of HA-tagged CRT3. (Fsk treatment for 1h)

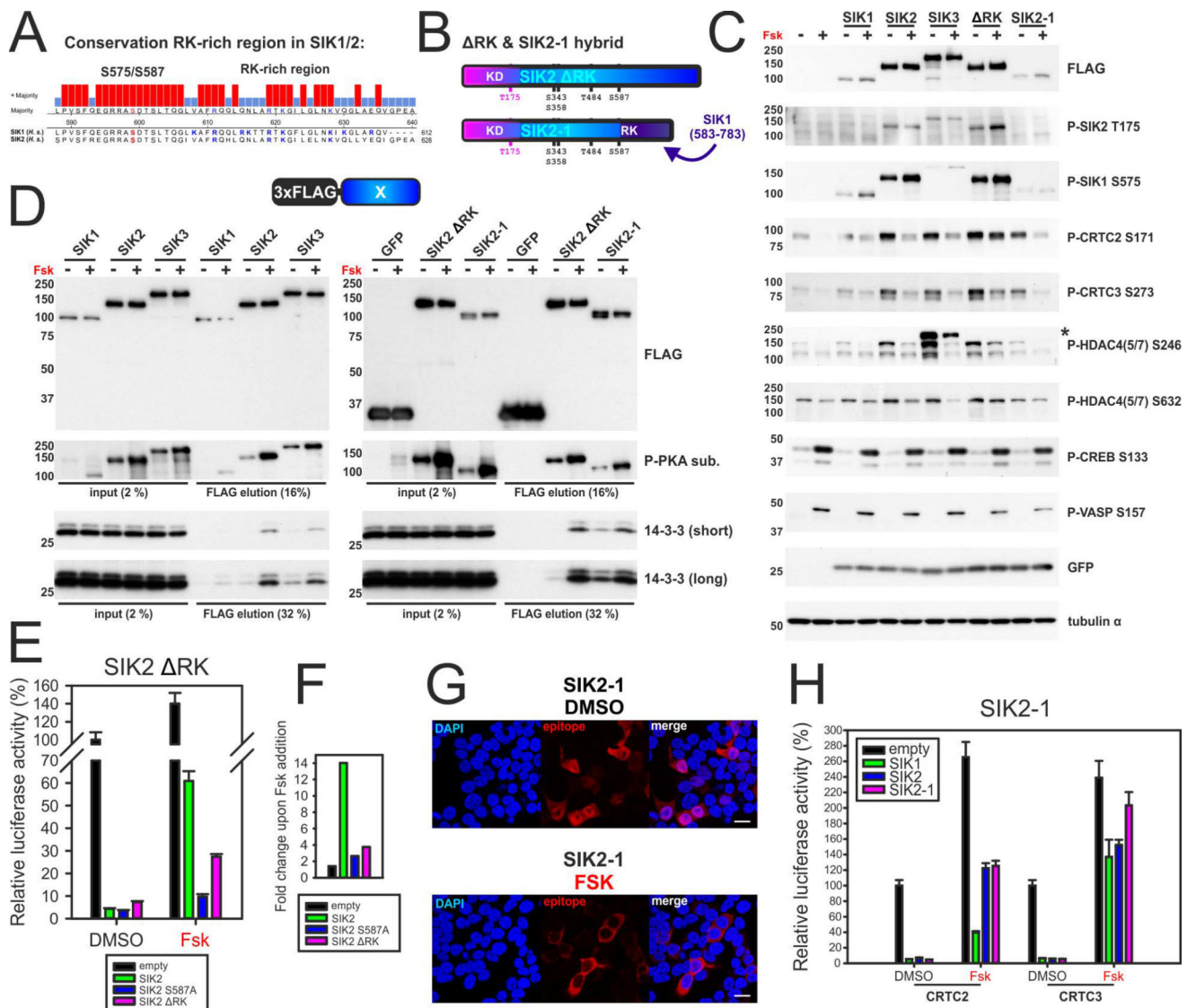


Fig. 5. The RK-rich of SIK1/2 modulates subcellular localization and cAMP-dependent kinase activity

A) Sequence alignment of *H. sapiens* SIK1 and SIK2. Depicted regions are the conserved PKA/14-3-3 site S575/S587 (SIK1/2) and the RK-rich region. Phosphorylated Ser (red) and Arg/Lys (blue) residues are highlighted. B) To scale schematic representation of SIK2 Δ RK and SIK2-1 hybrid proteins (SIK2 Δ RK = mSIK2 596–622, SIK2-1 = mSIK2 2–595 fused with hSIK1 583–783). C) Western blot analysis showing the effects of overexpressed FLAG-tagged SIK1–3, SIK2 Δ RK, and SIK2-1 on CRTC and class IIA HDAC phosphorylation. SIKs were expressed from a plasmid containing the constitutive Ubiquitin C promoter (UbC), which drives the expression of EGFP via an internal ribosome entry site (IRES). (* = cross-reactivity of overexpressed SIK3 with P-HDAC4(5/7) S246; DMSO/Fsk treatment for 1h) D) Western blot analysis of the Co-IP of FLAG-tagged SIK1–3 in comparison to GFP, SIK2 Δ RK, and SIK2-1 with endogenous 14-3-3 proteins. (DMSO/Fsk treatment for 1h) E) EVX-Luc reporter assay measuring the effect of SIK2 Δ RK upon the transcriptional activity of coexpressed CRTC3. EVX-Luc activity was measured after 4 h of DMSO/Fsk treatment.

(n = 5, \pm SEM) F) Graph depicting the corresponding fold changes in reporter activity upon Fsk treatment. G) Immunofluorescence of HEK293T cells transfected with FLAG-tagged SIK1 and SIK2-1 hybrid. Cells were stained for FLAG epitope and counterstained with DAPI. (DMSO/Fsk treatment for 30 min; scale bar indicates 20 μ m) H) EVX-Luc reporter assay measuring the effect of SIK1, SIK2, and SIK2-1 hybrid upon the transcriptional activity of coexpressed CRTC2 and CRTC3. EVX-Luc activity was measured after 4 h of DMSO/Fsk treatment. (n = 5, \pm SEM)

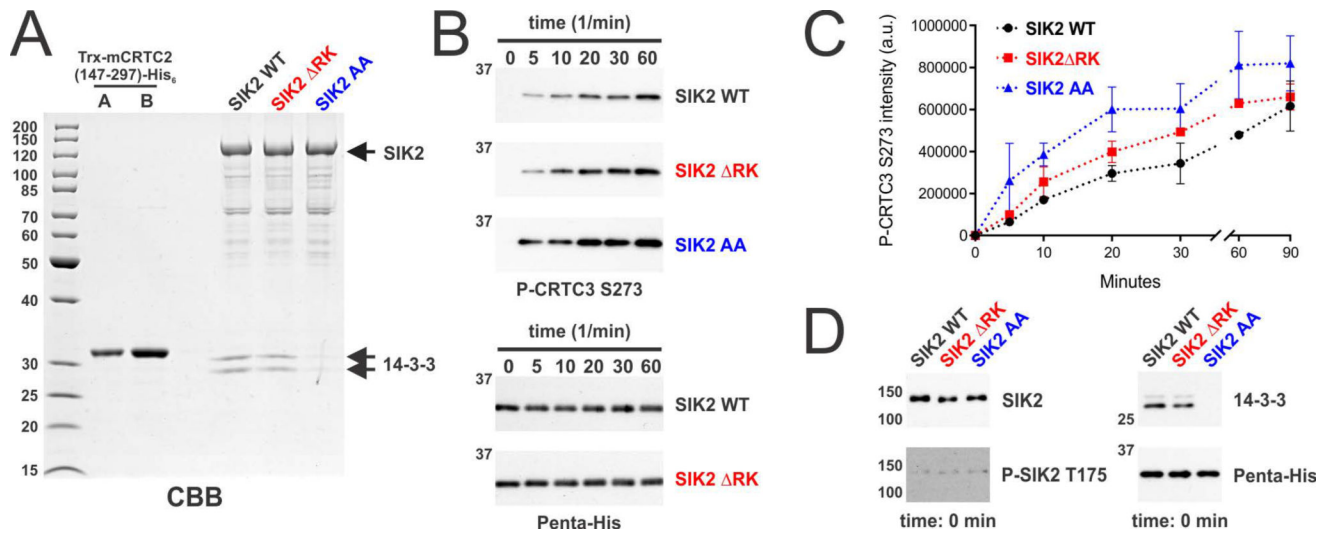


Fig. 6. *In vitro* SIK2 activity is modulated by 14-3-3 protein binding and RK-rich region mutants
 A) Coomassie brilliant blue (CBB) stained SDS page of heterologously expressed and purified Trx-mCRTC2(147–297)-His₆ (A = 0.5 μg and B = 1 μg). FLAG-SIK2 (WT, RK, and AA [S358A S587A]; all ~0.5 μg) were expressed in HEK293T cells and purified following Fsk exposure for 1h. B) The SIK2 kinase assay was performed using 0.05 μM SIK2 and 1 μM CRTC2 at 30 °C (see Material and Methods for details). Samples were taken at indicated time points, the reaction stopped by boiling in SDS sample buffer, and analyzed by Western blot. In the depicted sample SIK2 WT and SIK2 RK were analyzed on the same Western blot. In all experiments identical P-CRTC3 S273 antiserum dilution as well as exposure times were used. C) Graph plotting the densitometric analysis of the P-CRTC3 S273 antiserum intensity of two independent reactions. (n = 2, ±SD) D) Western blot analysis of the kinase assay at the 0-minute time point.

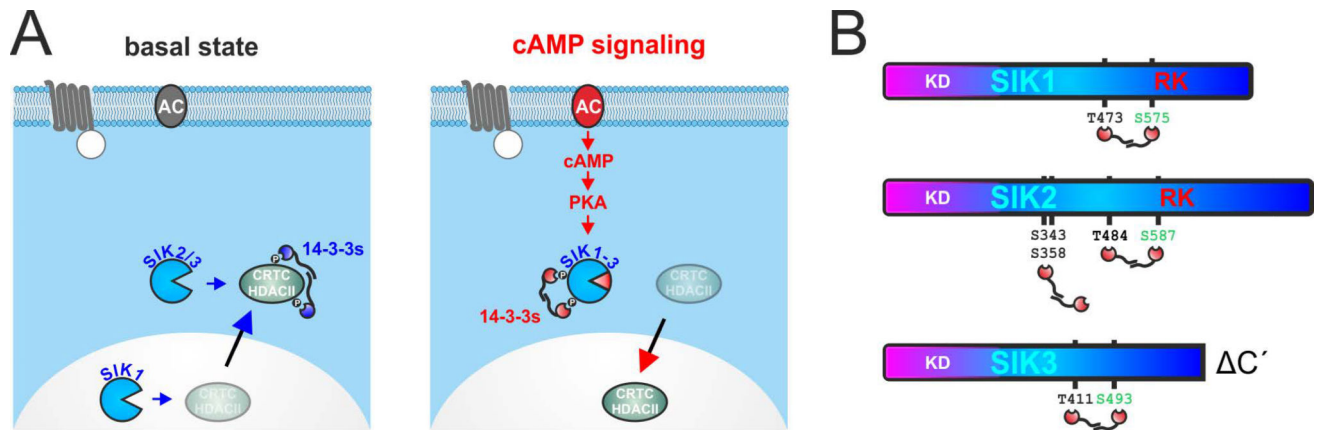


Fig. 7. Regulation of SIK activity by PKA-induced 14-3-3 binding

A) Scheme depicting the cAMP-regulated interplay of the SIK family with their canonical substrates cAMP-regulated transcriptional coactivators (CRTCs) and class IIA histone deacetylases (HDACs). Without stimulation, SIK-mediated phosphorylation sequesters CRTCs/HDACs in the cytoplasm by inducing 14-3-3 interactions (in blue). Upon cAMP stimulation, PKA-mediated phosphorylation inactivates the SIKs following 14-3-3 dimer association (in red; AC = adenylyl cyclase). In consequence, CRTCs/HDACs are dephosphorylated, lose 14-3-3s, and translocate to the nucleus. B) Schematic representation highlighting all functional 14-3-3 sites within the SIK family in black (two for SIK1/3 and four for SIK2) and the predominant sites in green (C' = SIK3's extended C-terminus isn't depicted). Although single phospho-acceptor mutant abolished cAMP sensitivity inside SIK1 and SIK3, additive effects between PKA/14-3-3 sites were observed for SIK2. Upon cAMP/PKA stimulation the conserved RK-rich region of SIK1/SIK2 is also required to convert 14-3-3 protein binding into catalytic inactivation.